TOXICOLOGICAL SCIENCES **106(2)**, 488–496 (2008)
doi:10.1093/toxsci/kfn183
Advance Access publication September 8, 2008

Dioxin Causes Ventral Prostate Agenesis by Disrupting Dorsoventral Patterning in Developing Mouse Prostate

Chad M. Vezina,* Sarah Hicks Allgeier,† Robert W. Moore,*,† Tien-Min Lin,* Jeffrey C. Bemis,‡ Heather A. Hardin,* Thomas A. Gasiewicz,‡ and Richard E. Peterson*,†,[1]

School of Pharmacy; †Molecular and Environmental Toxicology Center, University of Wisconsin, Madison, Wisconsin 53705; and ‡Department of Environmental Medicine, University of Rochester Medical Center, Rochester New York 14642

Received June 11, 2008; accepted August 21, 2008

Prostate ductal development is initiated by androgen-dependent signals in fetal urogenital sinus (UGS) mesenchyme that stimulate prostatic bud formation in UGS epithelium. 2,3,7,8-Tetrachlorodibenzo-*p*-dioxin (TCDD, 5 μg/kg maternal dose) inhibited ventral and dorsolateral but not anterior prostatic budding. We sought to determine which stage of budding, specification or initiation, was inhibited. Ventral prostatic bud formation was maximally inhibited when TCDD exposure spanned E15.5–16.5 and dorsolateral prostatic bud formation when it spanned E14.5–15.5. Because ventral and dorsolateral buds are specified at these times, TCDD impaired bud specification. We hypothesized that TCDD inhibited ventral bud specification by forming a continuous smooth muscle barrier between UGS mesenchyme and epithelium in the ventral prostatic UGS region, blocking mesenchymal-epithelial signaling, but no such barrier was found. We hypothesized that increased aryl hydrocarbon receptor (AHR) signaling in ventral and dorsolateral UGS increased their sensitivity to TCDD, but levels of AHR nuclear translocator (ARNT) protein, *Ahr* mRNA, and AHR-dependent gene expression were not higher than in anterior UGS where budding was unaffected. However, we identified overlapping expression of Ahr, ARNT, and AHR-induced transcripts in the periprostatic mesenchyme which intimately contacts UGS epithelium where buds are specified. This was considered the putative TCDD site of action in the UGS for inhibition of ventral and dorsolateral prostatic bud specification. Thus, hyperactivation of AHR signaling appears to disrupt dorsoventral patterning of the UGS, reprogramming where prostatic buds are specified, and prostate lobes are formed. Disrupted axial patterning provides a new paradigm for understanding how *in utero* TCDD exposure causes ventral prostate agenesis and may shed light on how TCDD impairs development of other organs.

Key Words: **dioxin; prostate; aryl hydrocarbon receptor.**

Prostate development begins prenatally when fetal androgens bind to androgen receptors in urogenital sinus (UGS) mesenchyme to stimulate prostatic ductal progenitors, or buds in UGS epithelium. Prostatic buds, like buds in other organs (Cohn and Tickle, 1996), are formed in sequential stages (Thomsen *et al.*, in press). The first stage is the specification stage, when molecular signals specify where buds will form on the UGS surface. Buds are specified along three asymmetric axes: dorsoventral, craniocaudal, and mediolateral. The second stage of bud formation is the initiation stage, when buds first project from the UGS epithelial surface. When C57BL/6J male fetuses were examined at 24-h intervals, anterior prostatic buds were first seen on embryonic day (E)16.5, the first dorsolateral buds were seen on E17.0, and ventral buds were first seen on E17.5. Prostatic bud initiation was completed by E18.5 yielding approximately 8 ventral, 48 dorsolateral, and 5–6 anterior buds (Lin *et al.*, 2003). Bud initiation is followed by the final stage of bud development, elongation, when buds extend distally into UGS mesenchyme. Most buds elongate, branch, canalize, and ultimately develop into the ductal network of the mature prostate that consists of three lobes: ventral, dorsolateral, and anterior (Sugimura *et al.*, 1986).

We found in C57BL/6J mice that 2,3,7,8-tetrachlorodibenzo-*p*-dioxin treatment (TCDD, 5 μg/kg maternal dose on E13.5) delayed prostatic bud initiation throughout the UGS, prevented ventral prostatic buds from forming, and decreased dorsolateral bud number (Lin *et al.*, 2003). TCDD acted directly on the UGS to inhibit prostatic budding (Lin *et al.*, 2004) in an aryl hydrocarbon receptor (AHR)–dependent fashion (Lin *et al.*, 2003). Inhibition of budding by TCDD required functional AHRs in UGS mesenchyme, not in UGS epithelium (Ko *et al.*, 2004a). Although prostatic budding required functional androgen receptors (ARs) in UGS mesenchyme (Cunha and Lung, 1978), impairment of ventral and dorsolateral budding by TCDD was not caused by reduced fetal testosterone or impaired AR transcriptional activity (Ko *et al.*, 2004b; Lin *et al.*, 2003).

The ventral and lateral UGS surfaces of TCDD-exposed mouse fetuses are devoid of epithelial outgrowths,

[1] To whom correspondence should be addressed at School of Pharmacy, University of Wisconsin, 777 Highland Avenue, Madison, WI 53705-2222. Fax: (608) 265-3316. E-mail: repeterson@pharmacy.wisc.edu.

demonstrating that TCDD interferes with prostatic budding by acting prior to the bud elongation stage (Lin *et al*., 2003). However, it was not known if TCDD inhibits budding by blocking bud specification, bud initiation, or both. Therefore, we sought to determine which of these early stages of prostatic bud formation is sensitive to TCDD. Mice were exposed to TCDD at 24-h intervals beginning before, during, or after bud specification and initiation, and prostatic budding was assessed at E18.5, after buds had formed. This study revealed that TCDD inhibits budding by impairing prostatic bud specification.

Differentiation of UGS mesenchyme into smooth muscle has been reported to create a barrier to paracrine signaling between UGS mesenchyme and epithelium essential for prostatic bud specification and/or initiation (Thomson *et al*., 2002). The most dramatic inhibitory effect of TCDD on bud formation is in the ventral UGS where no buds form. Focusing on this striking inhibition of ventral budding by TCDD, and knowing that there is a gap in the smooth muscle barrier in the ventral prostatic UGS, we sought to determine if TCDD causes this gap to close. If so, TCDD may effectively prevent mesenchymal-epithelial signaling that occurs across the smooth muscle gap in the ventral UGS to prevent ventral prostatic bud specification. Results of the present investigation show that TCDD does not cause the smooth muscle gap to close, dismissing this as a mechanism of action of TCDD.

A final objective was to test the hypothesis that ventral bud formation is the most susceptible to TCDD because AHR signaling is most abundant in the ventral region of the UGS. The distribution of *Ahr*, the AHR dimerization partner, AHR nuclear translocator (ARNT) (Reyes *et al*., 1992), and AHR-dependent gene expression was compared among ventral, dorsolateral, and anterior budding regions of the UGS. AHR signaling in the ventral region was not consistently more abundant than in dorsolateral or anterior regions. However, *Ahr*, ARNT, and three indices of AHR transcriptional activity were expressed in a specific region of UGS mesenchyme, designated "periprostatic UGS mesenchyme," defined as the mesenchyme closest to the UGS epithelium where prostatic bud formation occurs. The significance of these results is that they suggest that TCDD may impair prostatic bud formation by acting directly on the periprostatic UGS mesenchyme. We hypothesize that TCDD interferes with the signals that establish bud patterns along the dorsoventral UGS axis, resulting in ventral prostate agenesis and abnormal dorsolateral prostate development.

MATERIALS AND METHODS

Animals and treatments. All mice were maintained on a 12-h light/dark schedule with feed and tap water available *ad libitum*. C57BL/6J mice (The Jackson Laboratory, Bar Harbor, ME) were housed at 24 ± 1°C in clear plastic cages with corn cob bedding. Dams were fed 5015 Mouse Diet (PMI Nutrition International, Brentwood, MO), whereas weaned males were fed 8604 Rodent Diet (Harlan Teklad, Madison, WI). All procedures were approved by the University of Wisconsin Animal Care and Use Committee.

AHR-dependent *lacZ* reporter mice (Willey *et al*., 1998) were backcrossed to a C57BL/6J genetic background for more than 10 generations. These mice were maintained and treated in accordance with guidelines set by the University of Rochester Committee on Animal Resources and the American Association for Laboratory Animal Science. Animals were given food (5001 Rodent Diet; Purina Mills, MO) and water *ad libitum*.

Mice were bred by housing females overnight with males. E0.5 was defined as the morning after mating. In the initial experiment, pregnant mice were given a single oral dose of TCDD (5 μg/kg) or vehicle (corn oil, 5 ml/kg) on E13.5, 14.5, 15.5, 16.5, or 17.5. In all subsequent experiments, TCDD (5 μg/kg) or vehicle was given on E15.5. Dams were euthanized by CO_2 overdose. Fetuses were removed, placed in ice-cold phosphate-buffered saline (PBS) or Dulbecco's modified Eagle's medium, and bisected. Sex was determined by gonadal inspection.

In one experiment, pups remained with their mothers until postnatal day 21, at which time males were group housed (up to four per cage). Males were euthanized by CO2 overdose on postnatal day 90, and accessory sex organs were removed and weighed.

Scanning electron microscopy. UGS epithelium was imaged as previously described (Lin *et al*., 2003). Briefly, mesenchyme was manually removed from UGS after limited trypsin digestion. Epithelial samples were fixed with glutaraldehyde, dehydrated with graded ethanol, dried by the critical-point procedure, mounted, coated with gold, and viewed with a Hitachi S-570 scanning electron microscope (Hitachi, Tokyo, Japan). Scanning electron microscopy (SEM) was conducted at the University of Wisconsin Biological and Biomaterials Preparation, Imaging, and Characterization Laboratory.

In situ hybridization probes. An *Ahr* gene fragment was amplified from adult mouse prostate cDNA as described by Jain *et al*. (1998). *Cyp1b1* and *Cyp1a1* gene fragments were amplified from adult mouse prostate cDNA as described below. The primers used to amplify a 493-bp fragment of mouse *Cyp1b1* (positions +1156 to +1649 of Reference Sequence NM_009994) were 5′-ACTTCAGCAACTTCGTTCTGG-3′ and 5′-TGGGTCATGATTCACA-GACC-3′. The primers used to amplify a 1086-bp fragment of *Cyp1a1* probe (positions +886 to +1971 of Reference Sequence NM_009992) were 5′-TACCCAGCTGACTTCATTCCTGTC-3′ and 5′-GCCCAGGTATCTCC-TAACCCTTTC-3′. The *Ahr* fragment and *Cyp1a1* and *Cyp1b1* PCR products were subcloned into pCRII-TOPO. Vectors were linearized with *Hin*dIII and antisense riboprobes were synthesized with T7 RNA polymerase.

In situ hybridization. UGS were fixed in 4% paraformaldehyde prior to *in situ* hybridization. Some UGS tissues were embedded in 4% Seaplaque Agarose (Lonza, Rockland, ME) in PBS with 0.1% Tween-20 (PBT) and sectioned in ice-cold PBT using a Vibratome Model 1000 (Vibratome, St. Louis, MO) fitted with a Wilkinson Sword classic double-edge blade (Wilkinson Sword, Warner-Lambert Co., Milford, CT). The remaining tissues were analyzed in whole-mount. Whole-mount and sectioned UGS tissues were bleached in 6% H2O2 and digested at room temperature with 50 μg/ml proteinase K. Prehybridization (2 h) and hybridization (overnight) were each performed at 60.5°C. After high stringency washes, whole-mount UGS tissues were incubated overnight at 4°C in TBST (25mM Tris-HCl, pH 7.5, 140mM NaCl, 2.7mM KCl, 0.1% Tween-20) containing 5% sheep serum, and preblocked alkaline phosphatase-conjugated anti-digoxygenin. UGS tissue sections were incubated overnight in TBST containing 5% sheep serum, 1% bovine serum albumin, 1% blocking reagent (Roche, Indianapolis, IN), and alkaline phosphatase-conjugated anti-digoxygenin. The colorimetric reaction used BM Purple (Roche) as a chromogen. Additional methodological information about sectional ISH on UGS tissue sections is available in Supplemental File 1.

Immunohistochemistry. Tissues were fixed in 4% paraformaldehyde, dehydrated into methanol, infiltrated with paraffin, and cut into 5-μm sections. Sections were hydrated, bleached in 10% H2O2, and boiled in 10mM sodium citrate, pH 6.0, for 30 min. Tissues were washed with TBST. After blocking with normal sera (5%), tissue were incubated overnight at 4°C with blocking buffer containing rabbit anti-ARNT (1:100, Santa Cruz Biotechnology, Santa

Cruz, CA) or mouse anti-smooth muscle α-actin (1:50, Novocastra, New Castle, UK). Tissues were washed and incubated with biotinylated goat anti-rabbit IgG (for ARNT) or biotinylated anti-mouse IgG (Vector M.O.M. Peroxidase Kit [Vector Laboratories, Burlingame, CA], for smooth muscle α-actin), followed by streptavidin-conjugated horseradish peroxidase. Signal detection was achieved with the Vector NovaRED Peroxidase Kit as described by the manufacturer (Vector Laboratories). Sections were counterstained with hematoxylin.

Detection of AHR-dependent gene expression in UGS from lacZ reporter mice. AHR-dependent gene activation in UGS from *lacZ* reporter mice was visualized by examining the pattern of color that developed following incubation with the bacterial β-galactosidase substrate 5-bromo-4-chloro-3-indoyl-β-D-galactoside (X-gal) (Cheng *et al*., 1993). UGS were incubated in the X-gal staining solution for 3.5 h at 37°C in a humidified chamber, washed in PBS for 1 h, and postfixed in 70% ethanol. After photography, some UGS were dehydrated into ethanol, equilibrated in xylene, embedded in paraffin, sectioned at 25 μm, and counterstained with nuclear fast red. Others were rehydrated into PBT, embedded in agarose, and sectioned at 50 or 80 μm on a vibratome.

Litter independence and statistical analysis. SEM was generally conducted on UGS epithelium from three or more litters per time and treatment. Immunohistochemistry (IHC) was performed on UGS from three to five litters per time and treatment, whereas the number of litter-independent observations on UGS from AHR-dependent *lacZ* reporter mice was at least six. ISH was conducted on at least six litter-independent UGS per time and treatment.

Analysis of variance was conducted on untransformed or log-transformed dorsolateral and anterior prostate weight data that passed Levene's test for homogeneity of variance and appeared to be normally distributed. No significant effects were found. Due to the incidence of agenesis, ventral prostate weight was analyzed nonparametrically (Kruskal-Wallis ANOVA), followed by the distribution-free multiple comparisons test. Significance was set at $p < 0.05$. Results are presented as mean ± standard error.

RESULTS

The Specification Phase of Prostatic Bud Formation is Sensitive to TCDD

The various stages of prostate development are believed to be regulated by distinct molecular signals and occur at different stages of embryonic development (Thomsen *et al*., in press). We showed previously that *in utero* TCDD exposure starting on E13.5 inhibited ventral and dorsolateral prostatic bud formation (Lin *et al*., 2003). However, because TCDD causes sustained AHR activation, it was not possible to determine from that study whether budding impairment by TCDD was caused by AHR activation during bud specification or bud initiation. To identify which budding stage was sensitive to TCDD, male fetal mice were exposed *in utero* to vehicle (5 ml/kg corn oil) or TCDD (5 μg/kg, maternal dose) starting on E13.5, 14.5, 15.5, 16.5, or 17.5. This time course spanned bud specification and initiation stages, as shown in Figure 1. Prostatic buds were observed on E18.5 by treating UGS with trypsin, removing UGS mesenchyme with fine forceps, and visualizing the underlying UGS epithelium by SEM (Fig. 2). *In utero* TCDD exposure starting on E13.5 or E14.5 completely inhibited ventral bud formation, displaced dorsal and lateral buds toward the anterior UGS surface, and decreased dorsal bud number. *In utero* TCDD exposure starting on E15.5 inhibited ventral bud formation but partially restored dorsal and lateral bud position compared with E13.5 exposure. *In utero* TCDD exposure starting on E16.5 partially restored ventral bud number and further restored lateral bud position. *In utero* TCDD exposure starting on E17.5 fully restored the number and pattern of prostatic buds in all regions of the UGS. Thus, ventral bud formation was most sensitive to TCDD from E15.5 to 16.5, when ventral buds are specified. Dorsolateral bud formation was most sensitive to TCDD between E14.5 and 15.5, when dorsolateral buds are specified. Because these critical periods precede bud initiation (Fig. 1), TCDD impaired ventral and dorsolateral budding by interfering with bud specification and not initiation.

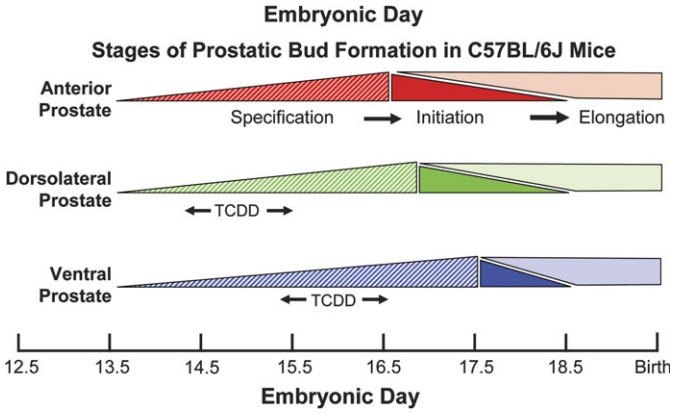

FIG. 1. Timing of the three prostatic bud formation stages: specification, initiation, and elongation for each prostate lobe. Approximate time frames of embryonic development when prostatic buds are specified, initiated and elongated in male C57BL/6J fetuses are illustrated for anterior (red), dorsolateral (green), and ventral buds (blue). The ''window of greatest sensitivity'' for inhibition of dorsolateral and ventral bud specification by TCDD is denoted by arrows.

We further interrogated the long-term effects of ventral bud agenesis. To confirm that TCDD exposure starting on E15.5 blocked ventral bud specification, rather than just delaying the formation of buds, we examined prostate weights in 90-day old adult mice ($n \geq 16$) that had been exposed *in utero* to TCDD starting on E15.5 or E16.5. *In utero* TCDD exposure at either time did not affect dorsolateral or anterior prostate weight. Fetal TCDD exposure starting on E15.5 caused ventral prostate agenesis, and TCDD exposure starting on E16.5 decreased ventral prostate weight by about 50% (Fig. 3).

Effects of In Utero *TCDD Exposure on Smooth Muscle Development in the UGS*

Thomson *et al*. (2002) postulated that smooth muscle restricts prostatic bud formation in male rat fetuses by acting as a barrier for paracrine signals traveling from UGS mesenchyme to UGS epithelium. They showed that smooth muscle circumscribes most of the male rat UGS but is absent from a gap of ventral UGS mesenchyme distal to the ventral

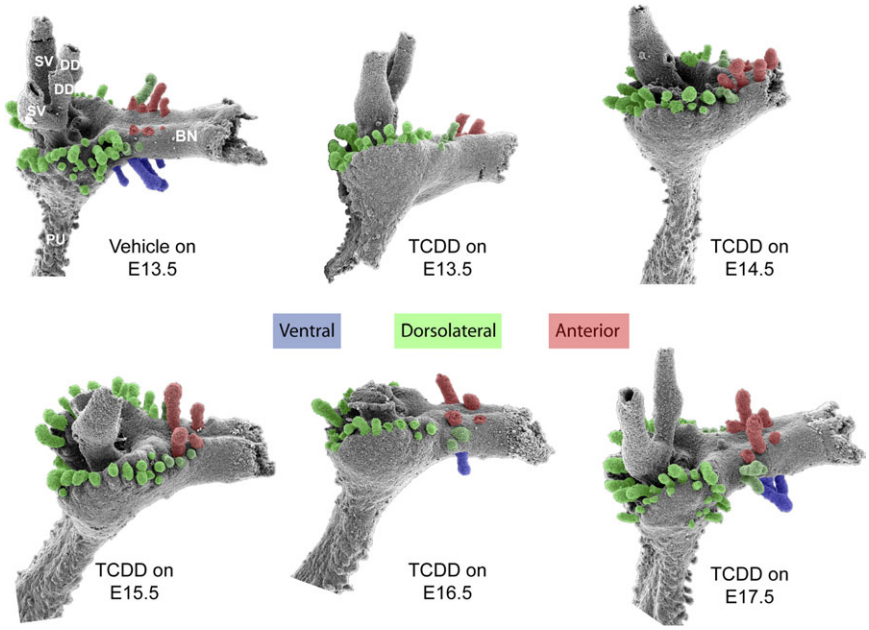

FIG. 2. Timing of fetal TCDD exposure influences the pattern and severity of prostatic bud inhibition by TCDD. Male fetal mice were exposed *in utero* to corn oil (vehicle, control) or TCDD (5 μg/kg, maternal dose) starting on embryonic day (E) 13.5, 14.5, 15.5, 16.5, or 17.5. UGS mesenchyme was removed from each UGS on E18.5 and underlying UGS epithelium was visualized by SEM. Results are SEM images of the lateral UGS epithelial surface and are representative of two to five UGS per group. Ventral prostatic buds are pseudocolored blue, dorsolateral buds are green, and anterior buds are red. Abbreviations: BN, bladder neck; DD, ductus deferens, PU, pelvic urethra, and SV, seminal vesicle.

budding region. We used IHC to visualize smooth muscle α-actin expression in mid-sagittal UGS tissue sections and test the hypothesis that TCDD prevents ventral prostatic budding by closing the ventral smooth muscle gap and blocking paracrine signals required for prostatic bud specification. Male fetal mice were exposed *in utero* to vehicle or TCDD (5 μg/kg maternal dose) starting on E15.5 and smooth muscle α-actin expression was assessed by IHC during ventral and dorsolateral bud initiation in E17.5 mouse UGS (Fig. 4). The pattern of smooth muscle α-actin was similar to that reported previously for rat UGS (Thomson *et al.*, 2002). We observed a multicellular band of smooth muscle α-actin that encircled the pelvic urethra and extended along the ventral prostatic UGS to the bladder, but was interrupted by a gap (Fig. 4, arrowhead) near the ventral prostatic budding zone. Smooth muscle α-actin was also absent from the anterior budding zone, but was present in a band of anterior UGS mesenchyme between the anterior budding zone and bladder. TCDD did not appear to affect the size of the ventral UGS smooth muscle gap or smooth muscle thickness in the ventral UGS mesenchyme, and did not qualitatively change abundance or distribution of smooth muscle in any other UGS region at E17.5.

Comparative Analysis of AHR Signaling in Ventral, Dorsolateral, and Anterior Prostatic UGS Regions

Rather than acting as a global inhibitor of prostatic budding, TCDD impairs bud specification in a graded fashion across the dorsoventral UGS axis: ventral UGS buds are blocked completely, dorsolateral buds are blocked partially, and some are displaced toward the anterior UGS surface, and anterior buds are spared by TCDD. We hypothesized that TCDD impaired bud specification in a graded fashion either because AHR signaling was unevenly distributed among UGS budding regions or because TCDD interfered with the mechanism of

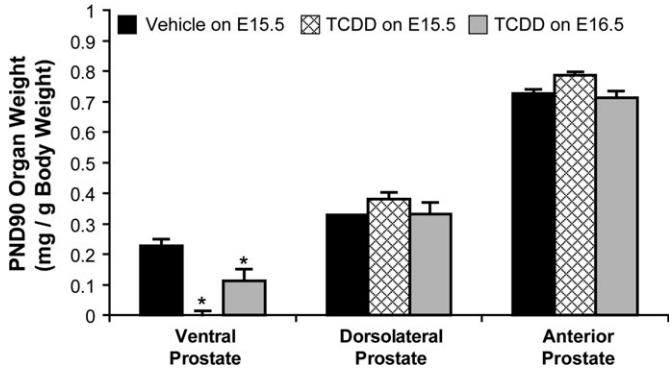

FIG. 3. *In utero* TCDD exposure on E15.5 causes ventral prostate agenesis, whereas TCDD exposure on E16.5 does not. Male fetal mice were exposed *in utero* to corn oil (vehicle, control) or TCDD (5 μg/kg, maternal dose) starting on embryonic day (E)15.5 or 16.5. Ventral, dorsolateral, and anterior prostate lobes were removed and weighed on postnatal day (PND)90. The weight of each lobe was normalized to total body weight. Results are mean ± standard error of the mean, $n = 16–28$ mice per group. An asterisk indicates a significant difference ($p < 0.05$) compared with control.

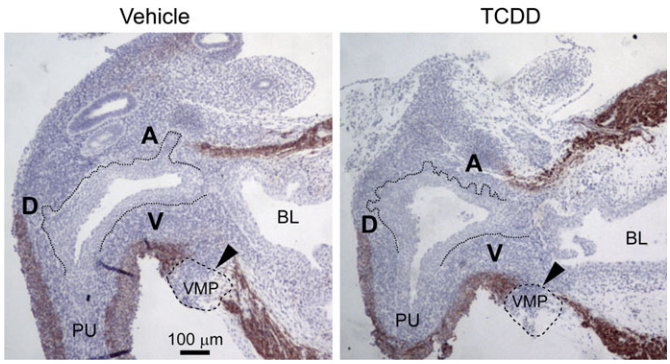

FIG. 4. TCDD does not close the smooth muscle gap in the ventral UGS. Male fetal mice were exposed *in utero* to corn oil (vehicle, control) or TCDD (5 μg/kg, maternal dose) on embryonic day (E)15.5. The pattern of UGS smooth muscle α-actin expression (red) was then visualized by IHC on E17.5. Dotted lines were added to demarcate the boundary between UGS epithelium and mesenchyme. Dashed lines circumscribe the VMP. The ventral (V), dorsolateral (D), and anterior (A) budding zones are labeled. Arrowheads point to ventral smooth muscle gap. Abbreviations: PU, pelvic urethra; BL, bladder.

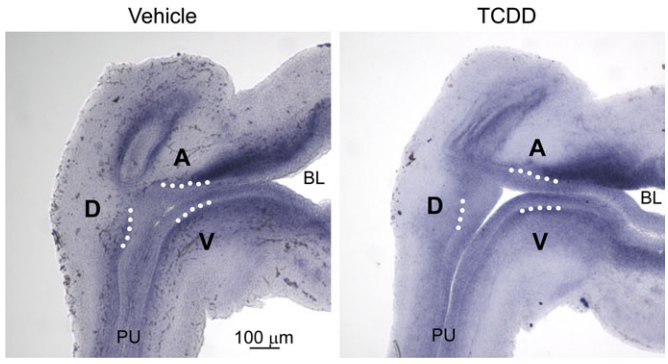

FIG. 5. *Ahr* mRNA expression in UGS from vehicle and TCDD-exposed male fetal mice. Male fetal mice were exposed *in utero* to corn oil (vehicle, control) or TCDD (5 μg/kg, maternal dose) on embryonic day (E)15.5. *In situ* hybridization was used to visualize the pattern of *Ahr* mRNA expression (shown in blue) in 80-μm sagittal UGS sections on E16.5. Results were representative of at least six males per group. Dotted lines were added to demarcate the boundary between UGS epithelium and mesenchyme in the ventral (V), dorsolateral (D), and anterior (A) budding zones. Abbreviations: PU, pelvic urethra; BL, bladder.

prostatic bud axial patterning. Our next objective was to determine whether ventral prostatic bud specification was the most sensitive to TCDD because of increased abundance of AHR or ARNT in the ventral prostatic UGS region compared with the dorsolateral and anterior budding regions. E15.5 male fetuses were exposed *in utero* to vehicle or TCDD and we used ISH to visualize *Ahr* mRNA distribution in whole-mount UGS tissues (not shown) and in sagittal UGS sections on E16.5 (Fig. 5). This exposure spanned the window of ventral bud specification most sensitive to TCDD. *Ahr* mRNA was detected in periprostatic UGS mesenchyme, and in epithelium in ventral, dorsolateral, and anterior budding zones. TCDD generally had little effect on *Ahr* expression and *Ahr* transcripts were not more abundant in the ventral UGS region compared with other budding regions in either vehicle- or TCDD-exposed samples.

Distribution of the AHR dimerization partner ARNT was determined by IHC also during the period of ventral bud specification (Fig. 6). ARNT was present in virtually every epithelial cell and most UGS mesenchymal cells on E16.5. ARNT expression was predominantly localized to cell nuclei and was distributed throughout all UGS budding and non-budding regions. *In utero* TCDD exposure did not qualitatively change ARNT abundance or distribution.

Three indices of AHR-mediated transcription were evaluated to test the hypothesis that ventral bud specification is more sensitive to TCDD because AHR activity is highest in the ventral UGS region. We evaluated TCDD-dependent β-galactosidase activity in the UGS of transgenic mice that harbor an AHR-responsive *lacZ* reporter gene (Willey *et al.*, 1998) and investigated TCDD-dependent induction of *Cyp1a1* and *Cyp1b1* in wild-type mice. Male fetuses were exposed *in utero* to vehicle or TCDD on E15.5 and β-galactosidase, *Cyp1b1*, and *Cyp1a1* distribution were measured 24 h later, on E16.5. We detected minimal constitutive β-galactosidase activity in UGS of vehicle-exposed transgenic mice (Fig. 7A). TCDD exposure on E15.5 induced β-galactosidase activity within 12–15 h (not shown); it was present at E16.5 (Figs. 7B and 7C) and persisted through at least E18.5 (Fig. 7D). UGS were stained and imaged as whole mounts (not shown) or serially sectioned through sagittal or transverse UGS planes to investigate β-galactosidase activity and its relation to ventral, dorsal, lateral, and anterior UGS budding regions. β-galactosidase activity was induced by TCDD in the periprostatic UGS mesenchyme, which was bounded by smooth muscle and UGS epithelium (Fig. 7E). The band of β-galactosidase activity in ventral UGS mesenchyme was most expansive in the mid-sagittal UGS plane and narrowed toward lateral UGS surfaces (Fig. 7C). β-Galactosidase activity was broadest in the ventral UGS budding region, where it extended outward into the ventral smooth muscle gap (Fig. 7E) and was most dense in part of the dorsal budding region (Fig. 7B). β-Galactosidase activity in UGS mesenchyme surrounded buds as they emerged from the UGS on E18.5, but did not focally increase or decrease in their immediate vicinity (Fig. 7D).

The pattern of AHR-responsive *Cyp1b1* mRNA expression in the UGS was investigated as another endpoint of AHR activity. *Cyp1b1* mRNA during ventral bud specification was expressed constitutively in E16.5 vehicle-exposed UGS. It was observed in portions of periprostatic mesenchyme circumscribing the UGS (Fig. 8). *Cyp1b1* was clearly induced by TCDD on E16.5. TCDD-induced *Cyp1b1* in periprostatic UGS mesenchyme in all UGS budding zones and the degree of induction appeared to be similar in all zones (Fig. 8). TCDD also induced *Cyp1b1* in UGS epithelium and in part of the ventral mesenchymal pad (VMP, an area of condensed

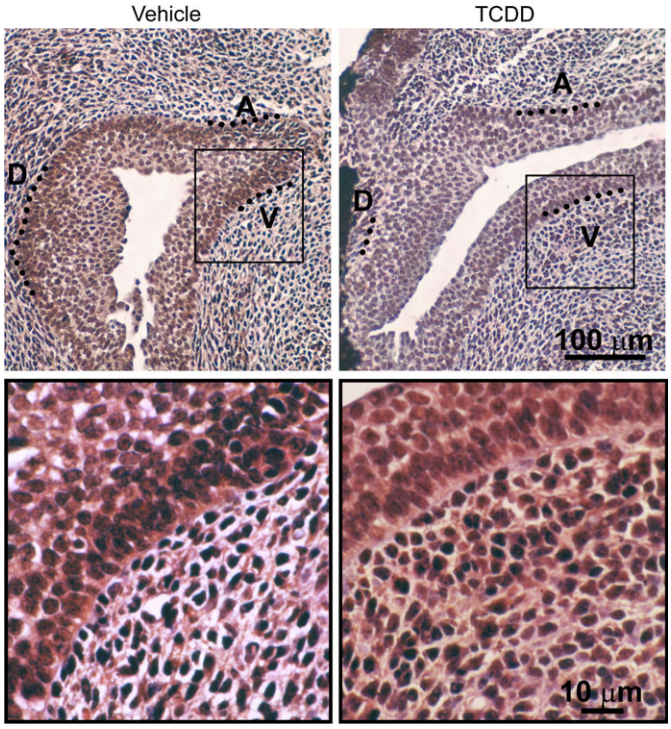

FIG. 6. ARNT protein expression in UGS from vehicle and TCDD-exposed male fetal mice. Male fetal mice were exposed *in utero* to corn oil (vehicle, control) or TCDD (5 μg/kg, maternal dose) on embryonic day (E)15.5. IHC was used to visualize the pattern of ARNT protein expression (red) in sagittal UGS sections on E16.5. Results are representative of at least three males per group. The ventral (V), dorsolateral (D), and anterior (A) budding zones are shown. A magnified image demonstrates that ARNT immunoreactivity is predominantly localized to nuclei of most cells, but is absent from some cells (blue).

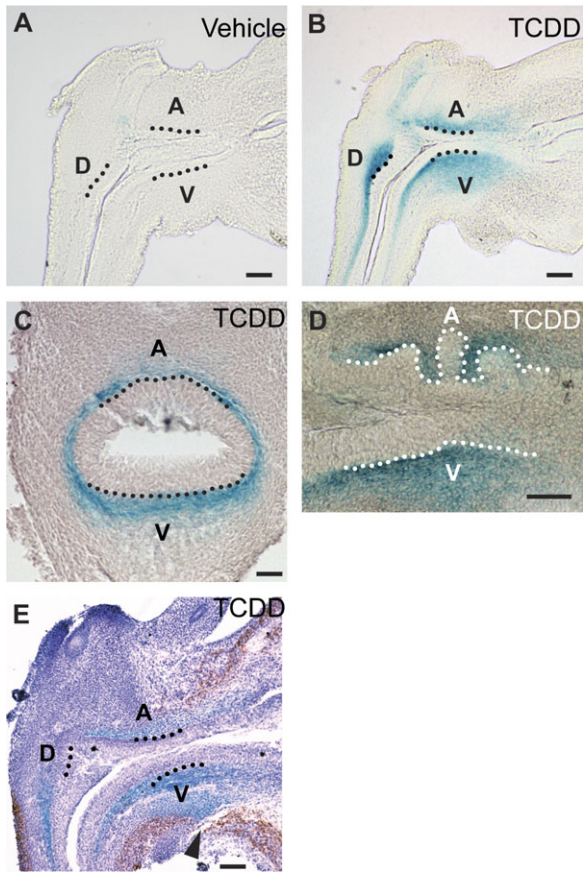

FIG. 7. AHR activity in the UGS of male AHR-responsive *LacZ* transgenic mouse fetuses exposed to vehicle or TCDD. Male fetal mice were exposed *in utero* to corn oil (vehicle, control) or TCDD (5 μg/kg, maternal dose) starting on embryonic day (E)15.5 and probed for β-galactosidase activity, shown in blue, on E16.5, 17.5 or 18.5. Results shown are representative of five UGS specimens per developmental time point. To evaluate AHR activity within specific UGS structures, β-galactosidase activity in UGS specimens was visualized by imaging of mid-sagittal sections from E16.5 (A) vehicle- or (B) TCDD-exposed mice, (C) transverse UGS sections from E16.5 (E) TCDD-exposed mice, or (D) sagittal sections from E18.5 TCDD-exposed mice. The relationship between smooth muscle and TCDD-induced β-galactosidase activity was determined by visualizing smooth muscle α-actin (red) by IHC in E17.5 UGS from TCDD-exposed *LacZ* transgenic mice. Dotted lines were added to demarcate the boundary between UGS epithelium and mesenchyme in the ventral (V), dorsolateral (D), and anterior (A) budding zones. The arrowhead points to the ventral smooth muscle gap. Scale bars = 100 μm.

mesenchyme distal to the smooth muscle layer). Although we did not colocalize *Cyp1b1* and smooth muscle α-actin in the same UGS samples, the band of ventral mesenchymal *Cyp1b1* induction that extended from ventral periprostatic mesenchyme to the VMP appeared to be in the vicinity of the smooth muscle gap.

The pattern of AHR-responsive *Cyp1a1* mRNA expression in the UGS was investigated as an additional endpoint of AHR activity. *Cyp1a1* mRNA was not detected in UGS from E16.5 vehicle-exposed mice (Fig. 9). However, *Cyp1a1* was induced substantially by TCDD in a multicellular layer of UGS epithelium near its interface with the sinus and to a much lesser extent in periprostatic UGS mesenchyme where anterior buds form and where ventral buds normally form (Fig. 9).

DISCUSSION

We showed previously that fetal and neonatal TCDD exposure decreased mouse prostate size (Lin *et al.*, 2002a) and we reported the extent to which *in utero* versus lactational TCDD exposure was responsible (Lin *et al.*, 2002b). We then showed that fetal TCDD exposure inhibited prostatic budding, thereby reducing the number of prostate ducts and causing a reduction in prostate size (Lin *et al.*, 2003). In the present study, we have further narrowed the developmental stage upon which TCDD acts to impair prostate development and have identified a potential mechanism of action: interference with prostatic bud specification. TCDD exposure between E15.5 and 16.5, during ventral bud specification, completely inhibited ventral bud formation and caused ventral prostate agenesis. TCDD exposure between E14.5 and 15.5, during dorsolateral

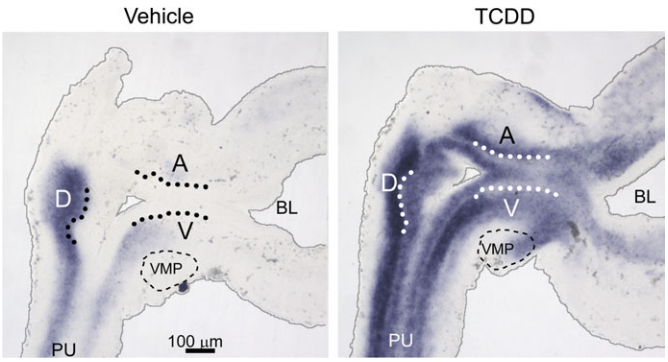

FIG. 8. *Cyp1b1* mRNA expression in UGS from vehicle and TCDD-exposed male fetal mice. Male fetal mice were exposed *in utero* to corn oil (vehicle, control) or TCDD (5 μg/kg, maternal dose) on embryonic day (E)15.5. *In situ* hybridization was used to visualize the pattern of cytochrome P450 1b1 (*Cyp1b1*) mRNA expression (shown in blue) in 50-μm sagittal UGS sections on E16.5. Results are representative of at least six males per group. Dotted lines were added to demarcate the boundary between UGS epithelium and mesenchyme in the ventral (V), dorsolateral (D), and anterior (A) budding zones, and thin gray lines were added to show the samples edges. Abbreviations: PU, pelvic urethra; BL, bladder.

bud specification, partially inhibited dorsolateral prostatic bud formation and caused some dorsolateral buds to form in a more dorsal position than normal. We showed previously that TCDD significantly decreased the number of main ducts in the dorsolateral prostate and inhibited its development (Ko *et al*., 2002; Lin *et al*., 2002a,b). We hypothesize that interference with how prostatic buds are specified contributes in part to the TCDD-mediated ventral prostate agenesis and inhibition of dorsolateral prostate development.

The formation of prostatic buds relies upon a basic developmental strategy: mesenchymal-epithelial communication.

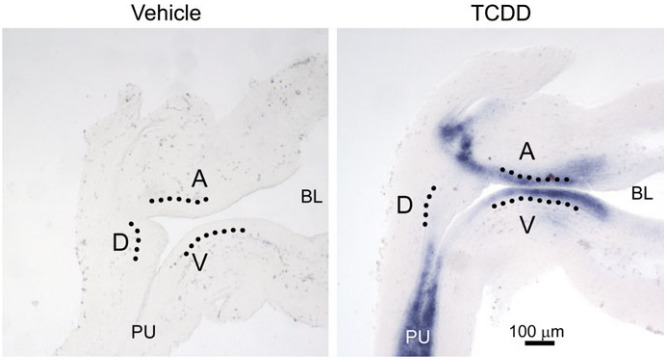

FIG. 9. *Cyp1a1* mRNA expression in UGS from vehicle and TCDD-exposed male fetal mice. Male fetal mice were exposed *in utero* to corn oil (vehicle, control) or TCDD (5 μg/kg, maternal dose) on embryonic day (E)15.5. *In situ* hybridization was used to visualize the pattern of cytochrome P450 1a1 (*Cyp1a1*) mRNA expression (shown in blue) in 50-μm sagittal UGS sections on E16.5. Results are representative of at least six males per group. Dotted lines were added to demarcate the boundary between UGS epithelium and mesenchyme in the ventral (V), dorsolateral (D), and anterior (A) budding zones. Abbreviations: PU, pelvic urethra; BL, bladder.

UGS mesenchyme permissively and instructively induces UGS epithelium to form prostatic buds (Hayashi *et al*., 1993). The results of the present study reveal that one of the areas in which TCDD activates AHR signaling is a particular layer of UGM tissue: periprostatic mesenchyme. Although *Ahr*, ARNT, and three different indices of AHR-inducible gene expression each exhibited somewhat different distribution patterns, their expression overlapped in all or at least portions of the periprostatic mesenchyme. Because this is the same tissue that specifies buds (Takeda *et al*., 1987), and TCDD impairs budding during the specification stage, we propose that inappropriate AHR activation by TCDD in periprostatic mesenchyme interferes with prostatic bud specification.

The pattern by which an organ develops in three dimensions is established by asymmetrically distributed morphogenetic signals that extend along the length of three different axes: craniocaudal, dorsoventral, and mediolateral (Meinhardt, 2008). These morphogenetic signals specify the pattern of prostatic buds. TCDD disrupts the pattern along one axis, the dorsoventral axis. This results in a dorsalized prostatic UGS characterized by a complete absence of buds on the ventral surface, severe reduction of buds on the lateral surface, and inappropriate clustering of buds on the dorsal surface.

One mechanism for this pattern of budding inhibition by TCDD is that AHR signaling is unevenly distributed across the dorsoventral prostatic UGS axis. The results of this study argue against this possibility. The abundance of *Ahr*, ARNT, and AHR-inducible gene expression was not greater near the ventral UGS region compared with the dorsal UGS region. In other words, we did not observe a dorsoventral AHR signaling gradient that would account for the dorsoventral pattern of budding inhibition by TCDD.

A major finding of the current study was that TCDD impaired prostatic bud formation by interfering with the specification stage of budding. Inasmuch as patterning signals are responsible for where buds are specified, the simplest explanation for the budding phenotype produced by TCDD is that AHR activation modulates dorsoventral patterning, thereby affecting bud specification along the dorsoventral axis. In support of this hypothesis, TCDD causes more prostatic buds to develop on the dorsal surface of the UGS than normal, no buds to form on the ventral surface, and few to develop on the lateral surface. However, this only occurs when the timing of TCDD exposure spans the period of prostatic bud specification. Also, the degree of dorsalization is influenced by the dose of TCDD. Buds are progressively lost in response to a graded increase in TCDD dose during bud specification: first from the ventral surface, next from the lateral surface, and at high doses from the anterior surface (Abbott *et al*., 2003). Exposure to TCDD after the dorsoventral axis has been established and bud specification has occurred has essentially no effect on the number or location of prostatic buds formed. Although our results show that AHR signaling is not itself asymmetrically distributed along the dorsoventral axis of the UGS, we propose

that its activation by TCDD interferes with the morphogenetic signaling gradients responsible for establishing and maintaining dorsoventral prostatic bud patterns.

We examined a possible mechanism by which TCDD impairs dorsoventral patterning. UGS mesenchyme contains a smooth muscle layer that is characterized by a gap in the ventral region. In control male fetal mice, this gap allows fibroblast growth factor 10 and other secreted morphogens to diffuse from the ventral axis pole dorsally toward the UGS epithelium where prostatic bud formation occurs. We tested the hypothesis that TCDD prevents ventral bud specification by enhancing smooth muscle proliferation in the ventral UGS to such an extent that it effectively closes the ventral smooth muscle gap. FGF10 is required for prostate development (Donjacour *et al*., 2003) and is synthesized by regions of condensed mesenchyme located specifically in the VMP and anterior UGS (Thomson and Cunha, 1999). Closing the smooth muscle gap in the ventral prostatic UGS of TCDD-exposed fetuses could prevent ventral buds from being specified and/or initiated. However, TCDD had no detectable effect on the thickness of the smooth muscle layer or the width of its ventral gap. We conclude that ventral bud agenesis in TCDD-exposed mice is due to factors other than effects on smooth muscle development.

We showed in the present study that AHR is transcriptionally active in part of the VMP, as evidenced by induction of *Cyp1b1* in this region. This was one of very few UGS regions where AHR activity extended distally from the periprostatic UGS mesenchyme. TCDD did not appear to cause a qualitative change in the size of the VMP, where *Fgf10* is synthesized, but it is possible that TCDD impairs *Fgf10* transcription or secretion and these possibilities are currently under investigation.

Hyperactivation of AHR signaling appears to disrupt dorsoventral patterning of the UGS, reprogramming where prostatic buds are specified and therefore where prostate main ducts are formed. This provides a paradigm for how *in utero* TCDD exposure causes ventral prostate agenesis and impairs dorsolateral prostate development. It is possible that this role of sustained AHR signaling may extend to other developing organs. Morphogen gradients are also involved in the induction of lung, molar, mammary, and salivary gland (Cardoso and Lu, 2006; Mikkola and Millar, 2006; Salazar-Ciudad, 2008; Tucker, 2007) and there is evidence that TCDD interferes with their development (Fenton *et al*., 2002; Kiukkonen *et al*., 2006; Kransler *et al*., 2007; Lin *et al*., 2001; Miettinen *et al*., 2002), but the genes and signaling pathways involved have not yet been determined. Disruption of axial patterning may explain how TCDD interferes with the normal development of these organs.

SUPPLEMENTARY DATA

Supplementary data are available online at http://toxsci.oxfordjournals.org/.

FUNDING

National Institutes of Health grants (R37 ES01332) to R.E.P., (F32 ES014284) to C.M.V., (F31 HD049323) to S.H.A., and (R01 ES09430 and P30 ES01247) to T.A.G.; and (T32 ES07015, T32 ES07026, and P50 DK065303).

ACKNOWLEDGMENTS

We thank Sharon Hildebrandt and staff for animal care at the University of Wisconsin, Nancy Proper for maintaining the *LacZ* reporter mouse colony at the University of Rochester, and Dr Ralph Albrecht for assistance with scanning electron microscopic imaging.

REFERENCES

Abbott, B. D., Lin, T.-M., Rasmussen, N. T., Albrecht, R. M., Schmid, J. E., and Peterson, R. E. (2003). Lack of expression of EGF and TGF-α in the fetal mouse alters formation of prostatic epithelial buds and influences the response to TCDD. *Toxicol. Sci.* **76,** 427–436.

Cardoso, W. V., and Lu, J. (2006). Regulation of early lung morphogenesis: Questions, facts and controversies. *Development* **133,** 1611–1624.

Cheng, T.-C., Wallace, M. C., Merlie, J. P., and Olsen, E. N. (1993). Separable regulatory elements governing myogenin transcription in mouse embryogenesis. *Science* **261,** 215–218.

Cohn, M. J., and Tickle, C. (1996). Limbs: a model for pattern formation within the vertebrate body plan. *Trends Genet.* **12,** 253–257.

Cunha, G. R., and Lung, B. (1978). The possible influence of temporal factors in androgenic responsiveness of urogenital tissue recombinants from wild-type and androgen-insensitive (Tfm) mice. *J. Exp. Zool.* **205,** 181–193.

Donjacour, A. A., Thomson, A. A., and Cunha, G. R. (2003). FGF-10 plays an essential role in the growth of the fetal prostate. *Dev. Biol.* **261,** 39–54.

Fenton, S. E., Hamm, J. T., Birnbaum, L. S., and Youngblood, G. L. (2002). Persistent abnormalities in the rat mammary gland following gestational and lactational exposure to 2,3,7,8-tetrachlorodibenzo-*p*-dioxin (TCDD). *Toxicol. Sci.* **67,** 63–74.

Hayashi, N., Cunha, G. R., and Parker, M. (1993). Permissive and instructive induction of adult rodent prostatic epithelium by heterotypic urogenital sinus mesenchyme. *Epithelial Cell Biol.* **2,** 66–78.

Jain, S., Maltepe, E., Lu, M. M., Simon, C., and Bradfield, C. A. (1998). Expression of ARNT, ARNT2, HIF1α, HIF2α and Ah receptor mRNAs in the developing mouse. *Mech. Dev.* **73,** 117–123.

Kiukkonen, A., Sahlberg, C., Partanen, A. M., Alaluusua, S., Pohjanvirta, R., Tuomisto, J., and Lukinmaa, P. L. (2006). Interference by 2,3,7,8-tetrachlorodibenzo-*p*-dioxin with cultured mouse submandibular gland branching morphogenesis involves reduced epidermal growth factor receptor signaling. *Toxicol. Appl. Pharmacol.* **212,** 200–211.

Ko, K., Moore, R. W., and Peterson, R. E. (2004a). Aryl hydrocarbon receptors in urogenital sinus mesenchyme mediate the inhibition of prostatic epithelial bud formation by 2,3,7,8-tetrachlorodibenzo-*p*-dioxin. *Toxicol. Appl. Pharmacol.* **196,** 149–155.

Ko, K., Theobald, H. M., Moore, R. W., and Peterson, R. E. (2004b). Evidence that inhibited prostatic epithelial bud formation in 2,3,7,8-

tetrachlorodibenzo-*p*-dioxin-exposed C57BL/6J fetal mice is not due to interruption of androgen signaling in the urogenital sinus. *Toxicol. Sci.* **79,** 360–369.

Ko, K., Theobald, H. M., and Peterson, R. E. (2002). *In utero* and lactational exposure to 2,3,7,8-tetrachlorodibenzo-*p*-dioxin in the C57BL/6J mouse prostate: Lobe-specific effects on branching morphogenesis. *Toxicol. Sci.* **70,** 227–237.

Kransler, K. M., Tonucci, D. A., McGarrigle, B. P., Napoli, J. L., and Olson, J. R. (2007). Gestational exposure to 2,3,7,8-tetrachlorodibenzo-p-dioxin alters retinoid homeostasis in maternal and perinatal tissues of the Holtzman rat. *Toxicol. Appl. Pharmacol.* **224,** 29–38.

Lin, T.-M., Ko, K., Moore, R. W., Buchanan, D. L., Cooke, P. S., and Peterson, R. E. (2001). Role of the aryl hydrocarbon receptor in the development of control and 2,3,7,8-tetrachlorodibenzo-p-dioxin-exposed male mice. *J Toxicol Environ Health A.* **64,** 327–42.

Lin, T.-M., Ko, K., Moore, R. W., Simanainen, U., Oberley, T. D., and Peterson, R. E. (2002a). Effects of aryl hydrocarbon receptor null mutation and *in utero* and lactational 2,3,7,8-tetrachlorodibenzo-*p*-dioxin exposure on prostate and seminal vesicle development in C57BL/6 mice. *Toxicol. Sci.* **68,** 479–487.

Lin, T.-M., Rasmussen, N. T., Moore, R. W., Albrecht, R. M., and Peterson, R. E. (2003). Region-specific inhibition of prostatic epithelial bud formation in the urogenital sinus of C57BL/6 mice exposed *in utero* to 2,3,7,8-tetrachlorodibenzo-*p*-dioxin. *Toxicol. Sci.* **76,** 171–181.

Lin, T.-M., Rasmussen, N. T., Moore, R. W., Albrecht, R. M., and Peterson, R. E. (2004). 2,3,7,8-Tetrachlorodibenzo-*p*-dioxin inhibits prostatic epithelial bud formation by acting directly on the urogenital sinus. *J. Urol.* **172,** 365–368.

Lin, T.-M., Simanainen, U., Moore, R. W., and Peterson, R. E. (2002b). Critical windows of vulnerability for effects of 2,3,7,8-tetrachlorodibenzo-*p*-dioxin on prostate and seminal vesicle development in C57BL/6 mice. *Toxicol. Sci.* **69,** 202–209.

Meinhardt, H. (2008). Models of biological pattern formation: From elementary steps to the organization of embryonic axes. *Curr. Top. Dev. Biol.* **81,** 1–63.

Miettinen, H. M., Alaluusua, S., Tuomisto, J., and Viluksela, M. (2002). Effect of *in utero* and lactational 2,3,7,8-tetrachlorodibenzo-*p*-dioxin exposure on rat molar development: the role of exposure time. *Toxicol. Appl. Pharmacol.* **184,** 57–66.

Mikkola, M. L., and Millar, S. E. (2006). The mammary bud as a skin appendage: Unique and shared aspects of development. *J. Mammary Gland Biol. Neoplasia* **11,** 187–203.

Reyes, H., Reisz-Porszasz, S., and Hankinson, O. (1992). Identification of the Ah receptor nuclear translocator protein (Arnt) as a component of the DNA binding form of the Ah receptor. *Science* **256,** 1193–1195.

Salazar-Ciudad, I. (2008). Tooth morphogenesis in vivo, in vitro, and in silico. *Curr. Top. Dev. Biol.* **81,** 341–371.

Sugimura, Y., Cunha, G. R., and Donjacour, A. A. (1986). Morphogenesis of ductal networks in the mouse prostate. *Biol. Reprod.* **34,** 961–971.

Takeda, H., Lasnitzki, I., and Mizuno, T. (1987). Change of mosaic pattern by androgens during prostatic bud formation in X^{Tfm}/X^{+} heterozygous female mice. *J. Endocrinol.* **114,** 131–137.

Thomsen, M. K., Francis, J. C., and Swain, A. (2008). The role of Sox9 in prostate development. *Differentiation* **76,** 728–735.

Thomson, A. A., and Cunha, G. R. (1999). Prostatic growth and development are regulated by FGF10. *Development* **126,** 3693–3701.

Thomson, A. A., Timms, B. G., Barton, L., Cunha, G. R., and Grace, O. C. (2002). The role of smooth muscle in regulating prostatic induction. *Development* **129,** 1905–1912.

Tucker, A. S. (2007). Salivary gland development. *Semin. Cell Dev. Biol.* **18,** 237–244.

Willey, J. J., Stripp, B. R., Baggs, R. B., and Gasiewicz, T. A. (1998). Aryl hydrocarbon receptor activation in genital tubercle, palate, and other embryonic tissues in 2,3,7,8-tetrachlorodibenzo-*p*-dioxin-responsive *lacZ* mice. *Toxicol. Appl. Pharmacol.* **151,** 33–44.